Effect of particle size on the electrocatalytic activity of platinum dispersions in carbon matrix electrodes for phosphoric acid fuel cells

S.-B. LEE and S.-I. PYUN*
Department of Materials Science and Engineering, Korea Advanced Institute of Science and Technology, 373-1 Kusong-Dong, Yusong-Gu 305-701, Taejon, Korea
(*author for correspondence, e-mail: sipyun@sorak.kaist.ac.kr)

Abstract

The loss in electrocatalytic activity of Pt particles in carbon matrix electrodes has been experimentally and theoretically investigated as a function of Pt particle size. The measurement of the cathodic potentiostatic current transient showed that a decrease in oxygen reduction current due to carboxyl group formation, relative to the oxygen reduction current in the absence of carboxyl group, increased with a decreasing Pt particle size. This relative value is a measure of the loss in specific activity. A model describing the electrocatalytic activity loss has been proposed by introducing a new parameter, characterising the effective dead active area produced by the carboxyl group formation, relative to the total active area free of the carboxyl group. The agreement of the experimentally determined relative current decrease with the calculated relative value of the effective dead active area confirms the model.

1. Introduction

Platinum-dispersed carbon (Pt/C) is used as a phosphoric acid fuel cell (PAFC) cathode catalyst. Over the last two decades, many studies [1–5] have focused on the corrosion of the carbon supports for Pt particles, since the corrosion of the carbon supports is one of the main causes of loss of electrocatalytic activity for oxygen reduction with time in a PAFC [6, 7]. At the operating potential for PAFC cathodes in the range of 0.7–0.9 V vs RHE, carboxyl group is a main constituent of the corrosion product on the carbon support. The formation potential E_f of a carboxyl group lies between 0.6 and 0.7 V vs RHE. Furthermore, it was shown that the carboxyl group formation and dissolution plays a major role in the decrease and enhancement of electrocatalytic activity of Pt/C catalysts, by reducing and increasing its active area, respectively [8].

Several authors [9–14] have reported that the specific activity of the catalyst decreases with a decreasing catalyst particle size. This is sometimes called the 'crystallite size effect'. In particular, they suggested that as Pt particle size decreases, the oxygen reduction rate decreases due to either the reduction in surface area of the Pt particles, that is, sintering effect [9], or to the increase in the interaction between Pt crystallites, that is, reduction in intercrystallite distance [11, 13]. In their study they should have also taken into account the corrosion of the carbon supports, because the loss in

electrocatalytic activity of the catalyst is also accompanied by the corrosion of the carbon supports.

Therefore, in the present work we investigated theoretically and experimentally the loss in electrocatalytic activity of a 10 wt% Pt/C catalyst as a function of Pt particle size in a 85% H_3PO_4 solution at 145 °C. For this purpose we introduced a parameter characterising the dead active area produced by the carboxyl group formation in the early stage of carbon corrosion, under operating conditions for the PAFC. At the same time we employed a potentiostatic current transient technique, X-ray diffractometry (XRD) and a transmission electron microscopy (TEM).

2. Experimental procedure

Platinum-dispersed carbon catalyst powder was heat-treated to various sized Pt particles from 300 to 800 °C for 2.5 h under a hydrogen and nitrogen mixture stream, with a flow rate of 500 sccm. Figure 1 shows a TEM micrograph of a 10 wt% Pt/C catalyst heat-treated at 800 °C for 2.5 h. The Pt particles are uniformly distributed over the carbon support and have spherical shape. Analysis of the X-ray diffraction patterns revealed that the diameter of Pt particles increased from 2.4 to 4.4 nm, on average, with an increasing heat treatment temperature. This result was in good agreement with that of the TEM analysis.
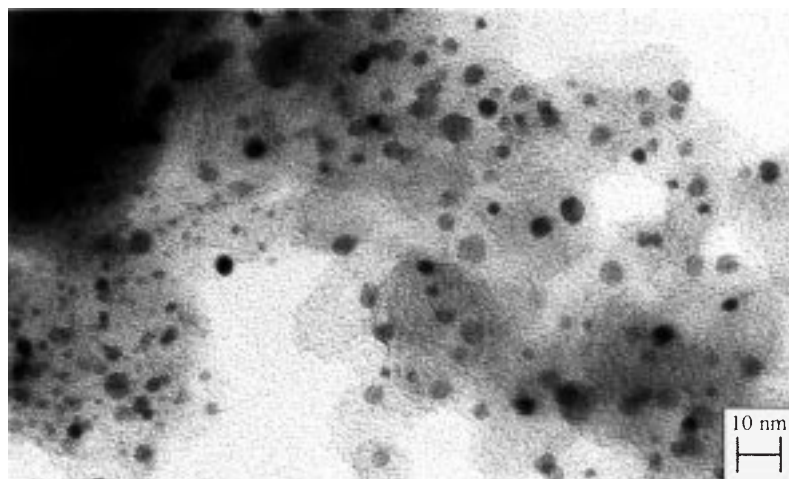
Fig. 1. TEM micrograph of 10 wt% Pt/C catalyst powder heat-treated at 800 °C for 2.5 h under hydrogen and nitrogen mixture stream.

The as heat-treated 10 wt% Pt/C catalyst powdered specimen was then prepared as a polytetrafluoroethylene (PTFE) bonded Pt/C electrode specimen, as detailed in a previous paper [8]. The various sized Pt-dispersed carbon electrode specimens were used as working electrodes. A platinum net and a reversible hydrogen electrode (RHE) were used as counter and reference electrodes, respectively. As electrolyte, we employed a 85% H_3PO_4 solution at 145 °C. The usual three electrode cell was constructed [5, 8].

The working electrodes were previously subjected to open circuit potential (OCP) of 0.9 V vs RHE for 1 h in 85% H_3PO_4 at 145 °C, followed by measurement of the cathodic current transient. To determine the oxygen reduction current as a measure of the electrocatalytic activity of the Pt/C catalyst, the cathodic potentiostatic current transient was measured on the Pt/C electrode by stepping the OCP to electrode potentials of 0.4, 0.6 and 0.8 V vs RHE. The electrochemical experiment was carried out using a potentiostat (EG&G PAR, model 263A).

3. Experimental results

Figure 2 illustrates the cathodic potentiostatic current transient resulting just after stepping the OCP of a 10 wt% Pt/C electrode down to 0.4 V vs RHE. In this Figure, the inverted L-shaped oxygen reduction current transient can be divided into two stages: in the first stage there is a rapid increase in current with time, and a linear increase in the second stage. This implies that the active area of Pt particles increase with time. The abrupt current increase in the first stage is due to the sum of the two contributions, the carboxyl group dissolution and the wetting of micropores, whereas, in the second stage the current increase is purely a result of one effect, the wetting of micropores. Conversely, when the OCP was stepped down to 0.6 V vs RHE, the first stage was not observed and only the second stage, which prevailed over the entire current transient, was noticed.

Our previous work [8] indicates that the carboxyl group already formed at the OCP around the Pt particles, is then dissolved during the first stage of the cathodic current transient at 0.4 V vs RHE. This enhances the active area of the Pt particles, and hence the oxygen reduction current. By contrast, the L-shaped cathodic current transient resulted from dropping the OCP to 0.8 V vs RHE. It was reported [8] that the rapid current fall in the first stage of the L-shaped current transient is most probably due to the dominance of the current fall by the carboxyl group formation over the current rise by the wetting of micropores.

In an attempt to quantitatively distinguish the increase in the oxygen reduction current with time caused by the carboxyl group dissolution, from the total first
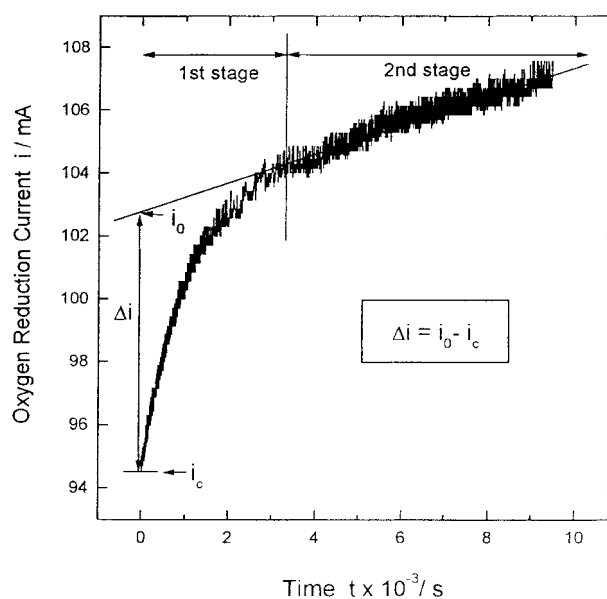

Fig. 2. Cathodic potentiostatic current transient measured on a 10 wt% Pt/C electrode by stepping the OCP to the electrode potential of 0.4 V vs RHE in 85% H_3PO_4 solution at 145 °C. i_0 represents second stage oxygen reduction current extrapolated to $t = 0$ and i_c means initial oxygen reduction current of the first stage at $t = 0$.

stage current transient, the linear increment with time in the second stage caused by the wetting of micropores should be subtracted from the total first stage current transient. As indicated in Figure 2, we obtained the difference in current, Δi, at $t = 0$, by subtracting the initial oxygen reduction current of the first stage i_c at $t = 0$ in the presence of carboxyl group around Pt particles, from the value of the second stage oxygen reduction current extrapolated to i_0 at $t = 0$. The value of i_0 is considered to be the oxygen reduction current in the absence of the carboxyl group around the Pt particles. Hence, the value of Δi is just the contribution of the carboxyl group dissolution to the oxygen reduction current increase. This can be regarded as being a measure of the loss in electrocatalytic activity of the Pt catalyst.

Figure 3 depicts the plot of $\Delta i / i_0$ as a function of Pt particle size r. The value of $\Delta i / i_0$ increased with decreasing particle size. This means that the loss in electrocatalytic activity increased with decreasing Pt particle size.

4. Theoretical considerations

4.1. *Ideal case for carboxyl group formation and dissolution*

First we consider the Pt particles uniformly distributed over the carbon support and a carboxyl group is formed at the OCP on the flat surface of the carbon support in the vicinity of the Pt particles. Next, we focus on one spherical Pt particle which is embedded in the surface of the carbon support. Then, we calculate the embedding depth, a, of a Pt particle as a displacement of the surface
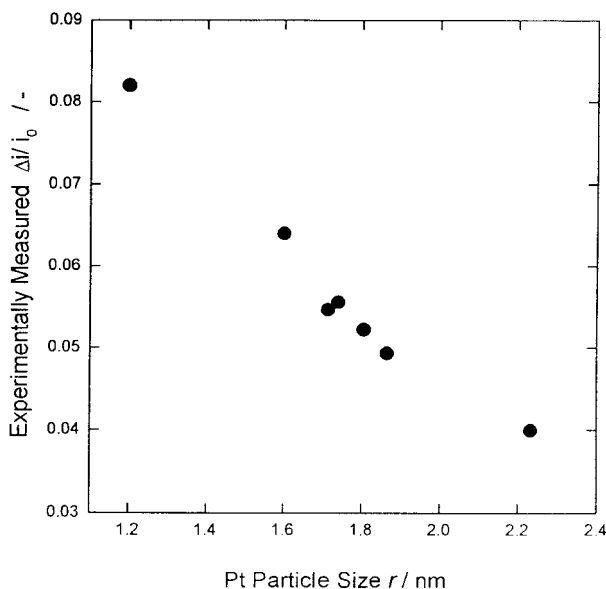

Fig. 3. Plot of the value of $\Delta i / i_0$ determined from the cathodic potentiostatic current transients obtained just after stepping the OCP down to 0.4 V vs RHE as a function of Pt particle size r.

level of the carbon support from the center of the embedded Pt particle. Thus, the value of a may range between $-r$ and r. Figure 4 schematically presents the carboxyl group formation around the Pt particle differently embedded in the flat surface of the carbon support for $0 < a \leq r$, $a = 0$ and $-r \leq a < 0$.

For the sake of simplicity, it is assumed that the carboxyl group layer grows to a monolayer thickness, d, in a direction perpendicular to the surface of the carbon support, in the vicinity of the Pt particle at the OCP. The monolayer of carboxyl group formed at the OCP is completely dissolved from the surface of the carbon support, by dropping the OCP to a potential lower than E_f.

In Figure 4, the total active area, A_0, represents the total surface area of the Pt particle that is exposed to the electrolyte in the absence of the carboxyl group coverage. The active surface area, A_c, is the surface area of the Pt particle that is exposed to the electrolyte in the presence of the carboxyl group coverage. The dead active area, ΔA, namely the circumferential band area of the Pt particle shaded by the carboxyl group coverage, is the difference between A_0 and A_c, $(A_0 - A_c)$.

However, in case where the value of a is between 0 and r, a crevice exists along the circumferential band because of the rectangular shape of the carboxyl group at the corner. Thus, as shown in the magnified view in Figure 4, the dead active area can be divided into two parts. The dissolved oxygen can penetrate through the electrolyte to the first part of the dead active area, which is termed the effective active area, A_c'. In contrast, the dissolved oxygen can scarcely penetrate through the electrolyte to the second part of the dead active area, which is termed the effective dead active area, ΔA_{eff}. As a result of the effective active area due to the crevice, we now introduce the effective dead active area, ΔA_{eff}, which is the difference between ΔA and A_c', $(\Delta A - A_c')$.

The dead area, that is, the dissolved oxygen-free electrolyte within the crevice, is actually determined by the critical permeable width, w, of the aperture for dissolved oxygen molecules, along with the effective layer thickness of the carboxyl group d_{eff}. The value of w should range, within at most, just one molecular diameter of oxygen. The value of d_{eff} is geometrically determined by the dimensions of w.

The relative value of the effective dead active area ΔA_{eff} to the total active area A_0, which is regarded as a measure of the loss in specific activity, can be expressed as

$$\frac{\Delta A_{eff}}{A_0} = \int_{a=-r}^{a=r} \frac{\Delta A}{A_0}(a) \frac{\Delta A_{eff}}{\Delta A}(a) f(a) \mathrm{d}a \tag{1}$$

where $\Delta A / A_0(a)$ is the ratio of the dead active area to the total active area as a function of the embedding depth a of a Pt particle; $s(a) = \Delta A_{eff} / \Delta A(a)$, the shading factor by the carboxyl group as a function of a, and $f(a)$
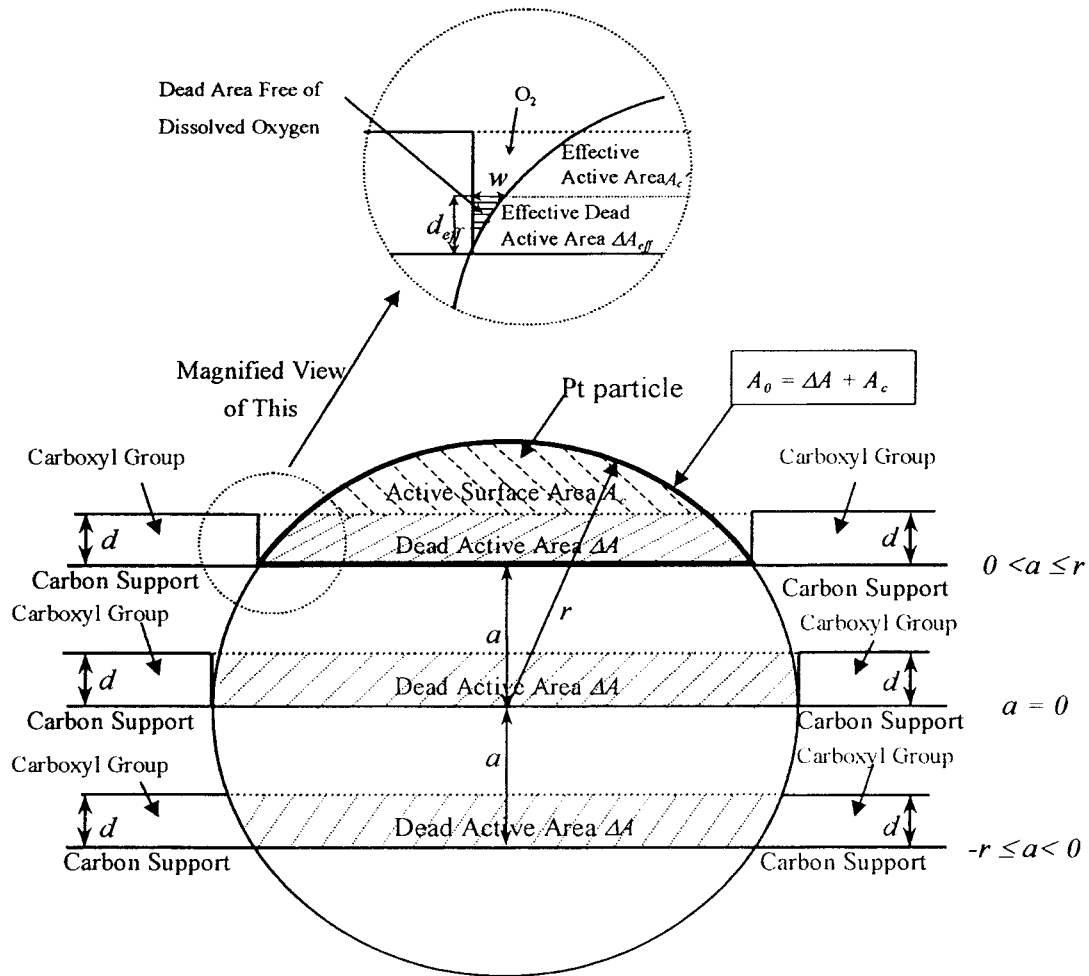
Fig. 4. Schematic diagram of the carboxyl group formation around a spherical Pt particle embedded in the flat surface of carbon support to $0 < a \leq r$, $a = 0$ and $-r \leq a < 0$. a = embedding depth of Pt particle, d = the layer thickness of carboxyl group, d_{eff} = the effective layer thickness of carboxyl group, w = the critical permeable width of aperture for dissolved oxygen molecule.

represents the distribution function of the embedding depth of the Pt particle. $f(a)\mathrm{d}a$ means the probability with which a Pt particle is embedded in the carbon supports, to a depth interval between a and $a + \mathrm{d}a$.

It is now necessary to obtain expressions for $(\Delta A/A_0)(a)$, $s(a)$, and $f(a)$ as a function of a, for a given Pt particle size r, at a fixed layer thickness d of the carboxyl group, and a constant critical aperture width w for the permeation of dissolved oxygen molecules.

4.1.1. *Ratio of the dead active area to the total active area, $(\Delta A/A_0)(a)$*

From the simple geometrical considerations of Figure 4, A_0 and ΔA are now expressed as a function of a for a constant value of r and d. Hence, the ratio of ΔA to A_0 can be then readily calculated as

$$\frac{\Delta A}{A_0}(a) = 1 \quad \text{if } r - d < a \leq r \tag{2a}$$

$$\frac{\Delta A}{A_0}(a) = \frac{d}{(r - a)} \quad \text{if } -r \leq a \leq r - d \tag{2b}$$

Figure 5(a) gives the plot of $\Delta A/A_0$ against a, calculated from Equations 2(a) and (b).

4.1.2. *Shading factor by carboxyl group, $s(a)$*

In this work, a shading factor by the carboxyl group, $s(a)$, is defined as a ratio of ΔA_{eff} to ΔA. Let us consider $s(a)$ in the following two cases of $0 \leq a \leq r$ and $-r \leq a < 0$.

First, the value of $\Delta A_{\mathrm{eff}}/\Delta A$ is identical to that value of d_{eff}/d for $0 \leq a \leq r$, owing to the spherical symmetry of the Pt particle. Hence, in this range of a, $s(a)$ is expressed by

$$s(a) = \frac{\left[r^2 - \left(-(r^2 - a^2)^{1/2} + w\right)^2\right]^{1/2} - a}{d} \tag{3}$$

for a constant value of r and w, considering the geometrical relations in the maginified view in Figure 4. The value of $d_{\mathrm{eff}}/d = \Delta A_{\mathrm{eff}}/\Delta A$ increases with decreasing a at a constant value of r and w. Let us designate the a value when $s(a) = 1$, as a^*. In such a regime $0 \leq a \leq a^*$, $s(a)$ is larger than 1. In this regime, Equation (3) is of no
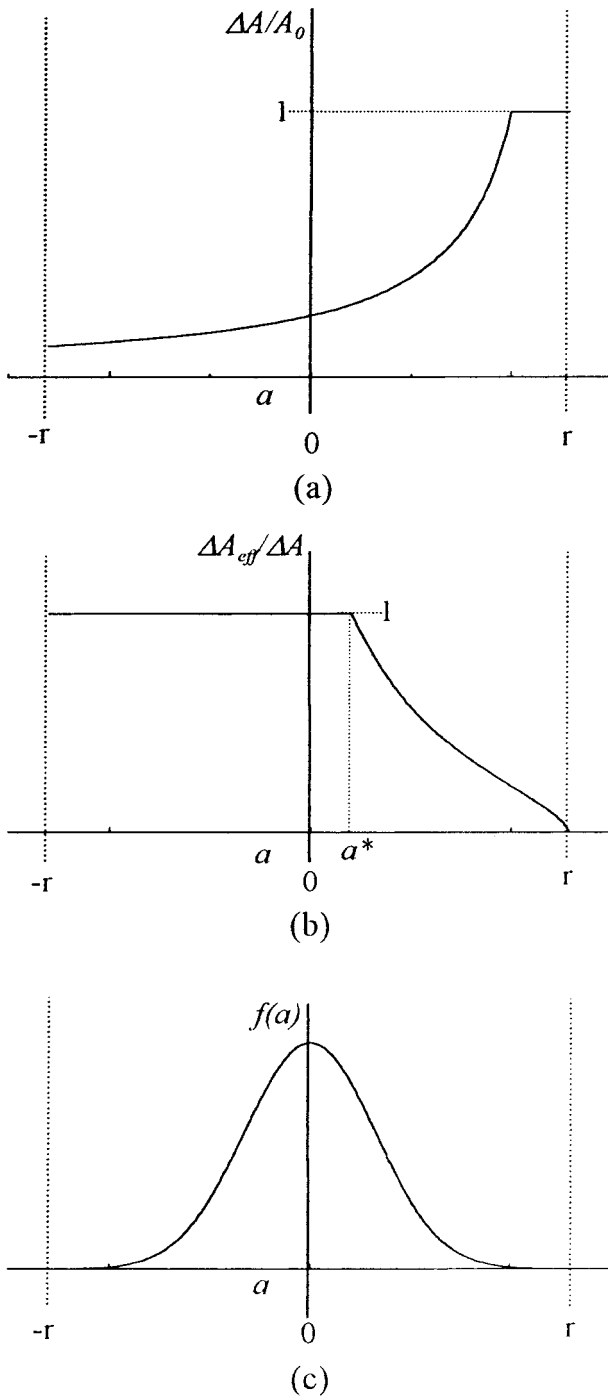
Fig. 5. Schematic representation of (a) $\Delta A/A_0$, (b) $\Delta A_{\text{eff}}/\Delta A$, and (c) $f(a)$ against embedding depth of Pt particle a. ΔA = the dead active area, A_0 = the total active area in the absence of carboxyl group, ΔA_{eff} = the effective dead active area, $f(a)$ = the normal probability distribution function.

physical significance, because ΔA is completely surrounded by the dissolved oxygen-free electrolyte, that is, the dead area free of dissolved oxygen. Thus the shading factor, $s(a)$, becomes unity.

The next step involves determining $s(a)$ for $-r \leq a < 0$. In this regime, the dead active area, ΔA, of the Pt particle is now completely covered with the carboxyl group, so that $\Delta A_{\text{eff}} = \Delta A$. Hence, $s(a) = 1$ for $-r \leq a < 0$.

Thus, the shading factor of the carboxyl group $s(a)$ is summarized as

$$s(a) = \Delta A_{\text{eff}}/\Delta A = d_{\text{eff}}/d \quad \text{if } a^* \leq a \leq r \qquad (4a)$$

$$s(a) = 1 \quad \text{if } -r \leq a < a^* \qquad (4b)$$

Figure 5(b) presents the plot of $s(a)$ against a, calculated from Equations 4(a) and (b).

4.1.3. Distribution function of Pt particle embedding depth, $f(a)$

In the present work, the value of a is assumed to obey a normal distribution, with zero as the mean value and $r/4$ as the standard deviation. Such a probability distribution function of a is given by

$$f(a) = \frac{1}{\sqrt{(2\pi)}\sigma} \exp\left(\frac{-(a-\mu)^2}{2\sigma^2}\right) \qquad (5)$$

where μ and σ represent the mean value and the standard deviation of a, respectively. Figure 5(c) envisages the plot of a normal probability distribution of embedding depth a, calculated from Equation 5.

4.2. Real situation of carboxyl group formation and dissolution

So far, we derived Equation 1 on the assumption that the carboxyl group forms to a monolayer thickness around the Pt particle at the OCP, and then the complete dissolution of this monolayer occurs from the surface of the carbon support around the Pt particle below E_f, as shown in Figure 4. However, in a real situation the carboxyl group formation proceeds at a very slow rate under the operating conditions for a PAFC. In addition, the carboxyl group dissolution is also a very sluggish process below E_f [8]. Therefore, we consider the following factors in modifying Equation 1.

4.2.1. Effects of an incomplete formation of the carboxyl group

In Section 4.1 we assumed that the carboxyl group layer is formed as a result of carbon corrosion during immersion at the OCP for 1 h, then grows to a monolayer thickness so that it covers the entire surface of the carbon supports in the vicinity of the Pt particle. However, it is actually conceivable that the surface of the carbon is not completely covered with the carboxyl group layer since the carboxyl group layer does not sufficiently grow to a monolayer thickness, due to its kinetically sluggish carbon corrosion. This means that the carboxyl group layer formed at the OCP amounts, on average, to between 0 and a monolayer thickness around the Pt particles.

4.2.2. Effects of the porosity of the carboxyl group

In Section 4.1 we assumed implicitly that the carboxyl group layer formed around the Pt particle is ideally

impermeable to dissolved oxygen molecules, thus blockading oxygen reduction on the Pt particle. However, in fact, the carboxyl group layer may probably contain such defects as small flaws and fissures, produced by carbon dioxide gas evolution in the later stage of carbon corrosion. Such defects give pathways for oxygen to migrate to the active sites of the Pt particle.

4.2.3. Effects of the incomplete dissolution of the carboxyl group

In Section 4.1, we assumed implicitly that all carboxyl groups formed at the OCP around a Pt particle can be completely removed from the surface of the carbon supports during the first stage of the current transient at 0.4 V vs RHE, as indicated in Figure 2. On the other hand, the current transients obtained just after dropping the OCP to 0.3, 0.4 and 0.5 V vs RHE showed that the value of $\Delta i/i_0$ slightly increases with falling electrode potential. This indicates that all carboxyl groups are not thoroughly dissolved during the first stage of the current transient in Figure 2, and hence a small amount of the carboxyl group still remains to a thickness ranging between 0 and a monolayer around Pt particles. Therefore all dead active sites of Pt particles are not perfectly converted into active sites for oxygen reduction below E_f.

4.3. Comparison between ideal and real cases for carboxyl group formation and dissolution

We now introduce a parameter v to effectively express those three effects described above on the value of $\Delta A_{eff}/A_0$. Thus, this new parameter is defined as the product of two probabilities. One is the probability to which an extent carboxyl group layer grows around Pt particles at the OCP, with respect to its ideal growth. In a similar way, the other is the probability to what extent the carboxyl group layer is dissolved from the vicinity of Pt particles below E_f, with respect to its complete dissolution. The value of v ranges between 0 and 1. In view of the real situation of the carboxyl group formation and dissolution, the value of $\Delta A_{eff}/A_0$ is reduced to

$$\frac{\Delta A_{eff}}{A_0} = v \int_{a=-r}^{a=r} \frac{\Delta A}{A_0}(a)\frac{\Delta A_{eff}}{\Delta A}(a)f(a)\mathrm{d}a \qquad (6)$$

Using the expressions for $(\Delta A/A_0)(a)$, $s(a)$ and $f(a)$ in Equations 2(a, b), 4(a, b) and 5, respectively, we can now calculate from Equation 6 the value of $\Delta A_{eff}/A_0$ for a given r. Considering the dimensions of the carboxyl group and oxygen molecules [15], the monolayer thickness d of a carboxyl group formed at the OCP, and the critical aperture width w for the permeation of dissolved oxygen molecules, are approximately estimated to be 0.3 nm and 0.2 nm, respectively. From the FTIR study [8] of the carboxyl group formation and dissolution, we can further roughly estimate the probability of the carboxyl group formation at the OCP and dissolution below E_f, to be 0.5 and 0.6, respectively.

Figure 6 depicts the plot of the value of $\Delta A_{eff}/A_0$, calculated based upon the model suggested above, as a function of a Pt particle size r that ranges from 1.1 to
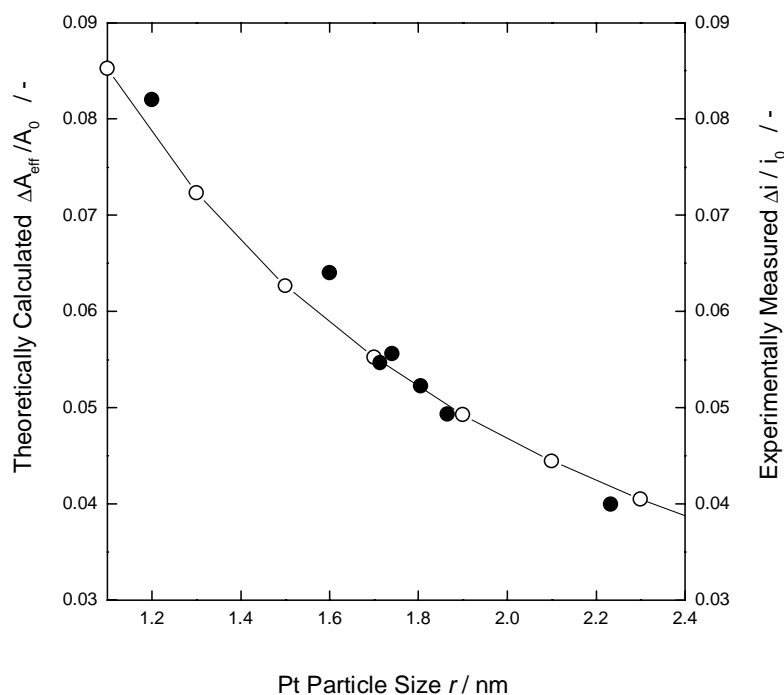

Fig. 6. Plot of the value of $\Delta A_{eff}/A_0$ theoretically calculated ($\bigcirc$) based on the model and that of $\Delta i/i_0$ experimentally measured ($\bullet$) against Pt particle size r.

2.3 nm, taking the parameters of $d = 0.3$ nm, $w = 0.2$ nm and $v = 0.3$. It is noted that by even adopting a probability distribution function other than the normal distribution function, we can also get approximately the same results as shown in Figure 6. The value of $\Delta i / i_0$, that is experimentally measured, as shown in Figure 3, is simultaneously registered in Figure 6 to compare it with that theoretically calculated.

From the comparison between the values of $\Delta i / i_0$ and $\Delta A_{eff} / A_0$, it can be seen that the plot of $\Delta i / i_0$ against r is in good agreement with that plot of $\Delta A_{eff} / A_0$ against r, in both shape and value. Thus, it turns out that the model is reasonable.

5. Conclusions

The experimental as well as the theoretical investigations of the loss in electrocatalytic activity as a function of Pt particle size r in a 85% H_3PO_4 solution at 145 °C, suggest the following conclusions:

(i) From both the measured FTIR spectra and the cathodic potentiostatic current transients, it is recognized that the value of the oxygen reduction current decrement Δi, due to the carboxyl group formation, relative to oxygen reduction current i_0 in the absence of the carboxyl group, increased with a decreasing Pt particle size r. The value of $\Delta i / i_0$ is regarded as being a measure of the loss in the specific activity.

(ii) According to the proposed model, the value of the effective dead active area ΔA_{eff} that is produced by the carboxyl group formation, relative to the total active area A_0 that is free of the carboxyl group, is expressed by multiplying the value of the dead active area ΔA, relative to the total active area A_0 by the two parameters of both the carboxyl group shading factor and the distribution of the embedding depth of Pt particles. The value of $\Delta A_{eff} / A_0$ was found to increase with a decreasing Pt particle size r. This relative value can be regarded as being a measure of the decrement of specific activity.

(iii) From the comparison of the value of $\Delta i / i_0$ experimentally determined, with that of $\Delta A_{eff} / A_0$ as theoretically calculated on the basis of the model, it can be seen that the measured plot of $\Delta i / i_0$ against r and the modelwise curve of $\Delta A_{eff} / A_0$ against r almost coincide in both shape and value. As a consequence, the decrease in specific activity with decreasing Pt particle size r, sometimes called the 'Pt crystallite size effect', can be understood in terms of the relative value of the effective dead active area developed by the carboxyl group formation.

Acknowledgements

References

1. K. Kinoshita and J.A. Bett, *Carbon* **11** (1973) 403.
2. K. Kinoshita and J.A. Bett, *Carbon* **12** (1974) 525.
3. P. Stonehart, *Carbon* **22** (1984) 423.
4. P.L. Antonucci, F. Romeo, M. Minutoli, E. Alderucci and N. Giordano, *Carbon* **26** (1988) 197.
5. S.-I. Pyun and Y.-G. Ryu, *J. Power Sources* **62** (1996) 1.
6. A.J. Appleby, *J. Energy* **12** (1986) 13.
7. A.J. Appleby and F.R. Foulkes, 'Fuel Cell Handbook' (Van Nostrand Reinhold, New York, 1989), p. 247.
8. S.-I. Pyun and S.-B. Lee, *J. Power Sources* **77** (1999) 170.
9. P. Stonehart, *Electrochim. Acta* **17** (1972) 2333.
10. L.J. Bregoli, *Electrochim. Acta* **23** (1978) 489.
11. M. Watanabe, H. Sei and P. Stonehart, *J. Electroanal. Chem.* **261** (1989) 375.
12. K. Kinoshita, *J. Electrochem. Soc.* **137** (1990) 845.
13. K. Yahikozawa, Y. Fujii, Y. Matsuda, K. Nishimura and Y. Takasu, *Electrochim. Acta* **36** (1991) 973.
14. A. Kabbabi, F. Gloaguen, F. Andolfatto and R. Durand, *J. Electroanal. Chem.* **373** (1994) 251.
15. D.R. Lide, 'CRC Handbook of Chemistry and Physics' (CRC Press, FA, 1994), p. 9–1.